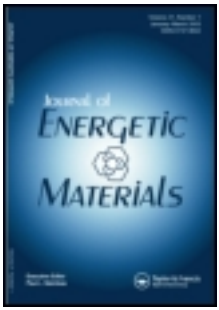

Journal of Energetic Materials
Publication details, including instructions for authors and subscription information:
http://www.tandfonline.com/loi/uegm20

Safety assessment studies of a damaged high-energy solid propellant

T. H. Zhang [a] , S. Y. Wang [b] & P. D. Liu [b]
[a] State Key Laboratory of Nonlinear Mechanics (LNM) , Institute of Mechanics, Chinese Academy of Sciences , Beijing, 100080, China
[b] Xi'an Modern Chemistry Research Institute , Xi'an, 710065, China
Published online: 25 Oct 2006.

To cite this article: T. H. Zhang , S. Y. Wang & P. D. Liu (2002) Safety assessment studies of a damaged high-energy solid propellant, Journal of Energetic Materials, 20:2, 175-189, DOI: 10.1080/07370650208244820

To link to this article: http://dx.doi.org/10.1080/07370650208244820

SAFETY ASSESSMENT STUDIES OF A DAMAGED HIGH-ENERGY SOLID PROPELLANT

T. H. Zhang

State Key Laboratory of Nonlinear Mechanics (LNM), Institute of Mechanics, Chinese Academy of Sciences, Beijing, China, 100080

S. Y. Wang, P. D. Liu

Xi'an Modern Chemistry Research Institute, Xi'an, China, 710065

ABSTRACT

This article presents a study of the effects of damage on the thermal decomposition, combustion and deflagration-to-detonation transition (DDT) of the NEPE (Nitrate Ester Plasticized Polyether) propellant in order to assess its safety. The study includes: (1) to induce damage into the propellants by means of a large-scale drop-weight apparatus; (2) to observe microstructural variations of the propellant with a scanning electron microscope (SEM); (3) to investigate thermal decomposition tests; (4) to carry out closed-bomb tests and (5) to perform DDT tests. The NEPE propellant is found to be a viscoelastic material. The matrices of damaged samples are severely degraded, but the particles are not. The results of the thermal decomposition tests, closed-bomb tests and DDT tests show that the microstructural damage in the propellant has some marked effects on its thermal decomposition rate, burn rate and transition rate from deflagration to detonation. It is shown that the impact damage strongly influences on safety properties of the NEPE propellant.

Journal of Energetic Materials Vol. 20, 175-189 (2002)
Published in 2000 by Dowden, Brodman & Devine, Inc.

INTRODUCTION

In order to meet the stringent performance requirements (i.e. range, payload, velocity) for the new generation of solid rocket motors, the amount of nitramine additives will be increased in the proposed chemical formulations of propellants. The two most common nitramines used to enhance propellant performance are 1,3,5-trinitro-1,3,5-triazacyclohexane (RDX) and 1,3,5,7-tetra-nitro-1,3,5,7-tetraza-cyclooctane (HMX). Unfortunately, the presence of these high-energy additives presents a trade-off between improved propulsion performance and the potential for an inadvertent explosion of rocket motors [1].

Some previous results have shown that the deflagration-to-detonation transition (DDT) of high-energy solid propellants sometimes occurs with a ballistic malfunction, which can heavily damage propellants. Since the propellants were consumed, little is known about the nature of the damage (generated under the stress fields) which leads to DDT. For instance, E. James and L. Green have reported the following result observed in a 155mm gun test [2]. DDT may occur after a primary shock of less than 1.0GPa has passed through the original cross-linked, double-base (XLDB) propellant, leaving behind changed regions that may be reduced to a fractured rubble. The hot spot population and surface area are thereby increased. Secondary shocks passing through damaged propellants at levels as low as 70MPa have initiated XLDBs.

Because of these problems and the evolution of safety regulations, it is now necessary to take safety issues into account at the very beginning of any project. Consequently, there is a need to develop laboratory techniques of small-scale tests to generate damaged propellant samples. These samples would be available for a variety of sensitivity and performance tests, such as augmented burning rate, closed tube DDT behavior and shock sensitivity.

The pyrotechnic behavior of solid propellants can be cataloged according to their chemical decompositions. Propellants may exhibit three modes of decomposition based on reactive speeds: thermal decomposition, combustion and detonation. Thermal decomposition is the first stage of the combustion process, combustion is a slower decomposition mode of propellants and detonation is the fastest decomposition mode. The aim of the present research is to examine and analyze the influences of damage on

the decomposition properties of the NEPE propellant. Therefore, the study consists of three parts: (1) to induce damage in the propellants, (2) to observe the microstructural changes, (3) to investigate if there is any difference in the thermal decomposition, combustion and DDT of the original and damaged propellants.

SAMPLE PREPARATION

Materials

The compositions of propellants tested here are listed in Table 1. RDX and AP(ammonium perchlorate) were used as the oxidizers. Al(aluminum powder) was used as the combustibility agent. NG(nitroglycerine) and BTTN(1,2,4-butanetriol trinitrate) were used as the plasticizer. PEG was used as the binder. N-100(hexane 1-6 diisocyanate homopolymer) was used as the crosslinking agent.

Table 1. Propellant compositions.

	Solid (75%)				Liquid (25%)		
Ingredients	RDX	AP	Al	catalyst	NG/BTTN	PEG	N-100
Weight (%)	40	16	18	1	19	5	1
Particle size (μm)	35	2/110	15/70	180			

Damage Production

In order to reduce the vulnerability of rocket systems to low velocity projectile/fragment impact or drop during transport, a fundamental understanding of the intermediate strain-rate behavior of the NEPE propellants is important. A hammer of 400kg mass in a large-scale drop-weight test dropped under gravity from a height of 0.25m to impact the sample. The processed propellants were machined into cylindrical samples of 40mm in diameter, 10mm in thickness. The apparatus and the typical load-time curve are shown in Fig. 1(a) and (b). In Fig. 1(b), the peak pressure p_m=145MPa is shown. The average axial strain-rate is $\dot{\varepsilon} = v/L = \sqrt{2gH}/L \sim 10^2 s^{-1}$.

From the observed stress-time curve (Fig. 1(b)), various deformation processes may occur. In Stage 1, extensive viscoelastic/plastic deformation occurs. In Stage 2, the sample was extensively crushed out and the pressure remained ca. 39MPa. In Stage 3, the pressure sharply increased. During impact, the sample underwent deformation so extensively that most of the sample was squeezed out from between the two Al plates and only a thin layer was left. After impact, the sample almost fully recovered, and cracks were not visible on the sample surface. This phenomenon implies that the propellant exhibits some characteristics of elastomeric polymers undergoing quasi-rubber-like deformation.

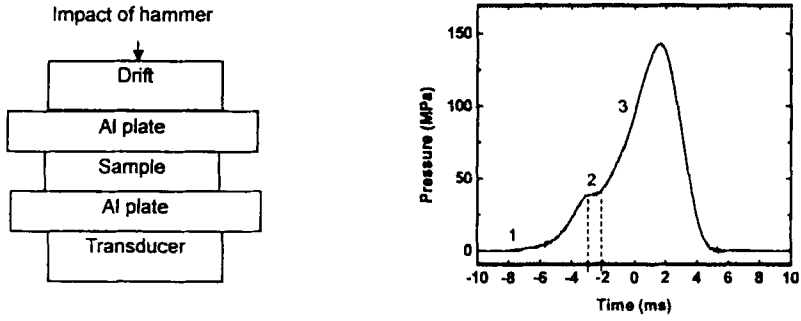

(a) (b)

Fig.1 (a)Schematic Diagram of Impact Test, (b)Load-Time Curve.

DAMAGE CHARACTERIZATION

Damage in the samples subjected to the drop weight loading was evaluated by means of scanning electron microscopy and density measurements.

Scanning Electron Microscopy (SEM)

The samples did not exhibit visible cracks. So, SEM was used to examine the sections of the original and impacted samples in order to identify damage modes under the impact condition.

Firstly, we should keep the following facts in mind. The NEPE propellant is an

energetic composition containing various particle sizes of RDX, AP and Al powders. Its matrix is made up from a great deal of energetic plasticizer nitrate ester (NG+BTTN) and polyurethane binder (PEG+N-100). The surface of a RDX crystal is inert so that RDX crystals in the propellant were weakly bonded to the matrix.

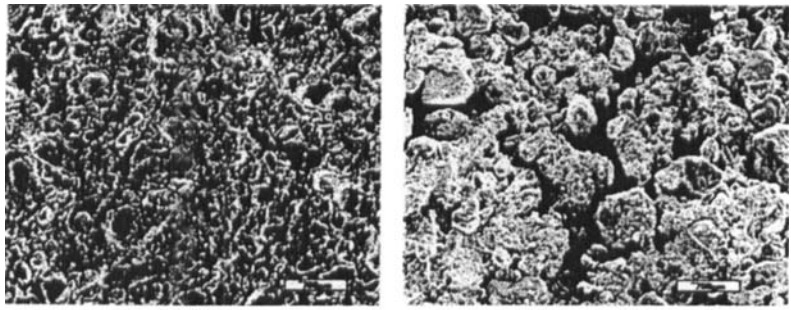

(a) 100× (b) 100×

Fig. 2 (a) The Original Sample, (b) The Impacted Sample.

The SEM micrograph from a microtomed cross-section of the original sample is shown in Fig. 2(a). The polyurethane binder adhered to the crystal surfaces of filled RDX particles poorly. For instance, there are seams in the range of $10^0\mu m$-$10^1\mu m$ between RDX particles and the matrix. Thus, the bigger RDX particles easily went apart at the seams. In order to improve the adhesive properties of the matrix and the filled particles, a suitable binding agent should be used or the filled particles should be coated to restrain dewetting.

Compared to the original samples, the impacted samples show changes (see in Fig. 2(b)) in two ways: (1) The matrix was torn. Between the bigger particles and the voids in the matrix, a great many microcracks formed and propagated. (2) Bigger particles dewetted. The bigger particles were separated from the matrix, but the particles themselves were not disrupted. At the same time, smaller particles were still coated with the matrix.

THERMAL DECOMPOSITION TESTS

The combustion process includes several steps from condensed phase to gas phase,

in which the condensed phase plays an important role. The reaction in the condensed phase is thermal decomposition. Thermal decomposition is the first step of combustion. Therefore, a thorough and detailed investigation of the thermal decomposition of the propellant should be performed as a basis of combustion.

The measurements were performed on a DSC 910 instrument, made in American TA Corp., at a heating rate of 10K/min and with a nitrogen flow rate about 40cm^3/min, and samples weighed about 1mg~5mg. The other measurements were carried out on a TGA 2950 instrument, made in American TA Corp., at a heating rate of 5 K/min and with a nitrogen flow rate of 60cm^3/min. 1mg~5mg samples were put in an aluminum cell.

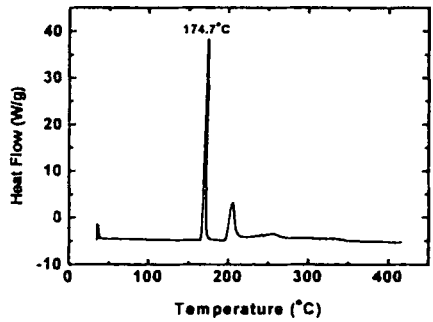

(a)

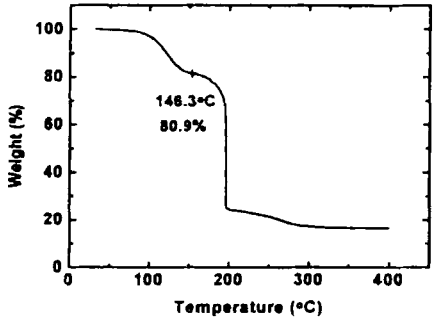

(b)

Fig. 3. The Original Sample (a) DSC Curve and (b) TG curve.

Table 2. Results for Thermal Decomposition of the Nitrate Ester.

Methods	DSC	TG
Characteristic Variables	T_p(℃)	ΔG(%)
Original sample	174.7	19.1
Impacted Sample	173.2	21.6

For original sample, typical DSC (Differential Scanning Calorimetry) and TG (Thermogravimetry) traces are shown in Fig. 3. Table 2 gives decomposition peak temperature T_p and mass loss % ΔG of the nitrate ester in the propellant.

On the DSC curve, there are three exothermic peaks, which have been assigned to three marked decomposition ranges. The first exothermic peak is decomposition of the nitrate ester, and emerges at about 170 ℃. The second is the oxidizer RDX's decomposition and appears at about 200℃. The third is the oxidizer AP's decomposition at about 250℃, and there exists an endothermic peak at about 240℃, which is a crystal transformation of AP.

The TG curve of the propellant is divided into three stages. The temperature range for the first mass loss stage is in the range of about 80℃~150℃, and the mass loss percent (about 19.1%) is equal approximately to the mass of plasticizer nitrate ester(NG/BTTN). So, it is mainly the volatilization and decomposition of nitrate ester. When the temperature increases continuously, RDX and a little of AP decomposed. In addition, the mass loss % increases quickly, and the decomposition is at about 200℃. In the third stage, a great deal of heat is released by the dissolved energetic components (NG+BTTN, RDX, AP). The degradation of polyurethane is initiated while the degradation promotes the decomposition of the surplus AP. The above analysis is supported by previous published papers [4,5]. The residues are mainly Al_2O_3, which are produced owing to the burning of Al powders.

For impacted sample, the decomposition peak temperature and mass loss rate of the impacted sample are listed in Table 2. For the impacted sample, the decomposition process is approximately consistent with the observations for the original sample. Only a few minor differences were observed and they focus on T_p and ΔG of the nitrate ester. In contrast to the original sample, in DSC, the T_p of the nitrate ester of the impacted sample

is shifted slightly to a lower temperature. It can be explained by the decreased activation energy of the nitrate ester due to its destroyed structure. On the other hand, in TG, ΔG increased. Likewise, this can be contributed to the reduction in activation energy. As shown in DSC and TG, the impacted sample is less thermally stable than the original sample.

CLOSED-BOMB TESTS

Both impacted and original samples were cut with a microtome into regular 5mm×5mm×5mm cubic grains. Then, a 90.75cm^3 (34mm in diameter, 10mm in length) closed-bomb was used to burn the same amount of cut cubes with total weight of 18.9g, respectively. The ignition primer for these tests consisted of 1.1g NC (nitrocellulose), which was ignited via an electric fuse. The chamber pressure was monitored as a function of time with a 500MPa quartz piezoelectric pressure gage, and charge-amplified signals were transmitted to a digital oscilloscope. The data of voltage versus time were stored on floppy diskettes and converted to ASCII format for burn property analysis.

In Table 3, t_m denotes the time reaching maximum pressure p_m and t denotes the time to reach maximum pressurization-rate $(dp/dt)_m$. Table 3 outlines the results of closed-bomb tests on the original and impacted samples. The curves for pressure-time (p-t) and pressurization-rate-time (dp/dt-t) are presented on Fig. 4. The solid and dotted lines correspond to the experimental data of the impacted and original samples, respectively. In comparison with the original sample, the combustion process of the impacted sample demonstrates distinct changes see Fig. 4(a) and Fig. 4(b), namely, t_m and t of the impacted sample drop 13.6% and 27.8%, respectively. The results can be explained by the dependence of the burn rate on the ratio of surface-to-volume. In fact, the impact loading induced a great many microcracks in the microstructure of the sample. These microcracks can even be seen after unloading (Fig. 2(b)) and increase the ratio of surface to volume in the impacted sample.

Table 3. Results for the Closed-bomb Tests.

	p_m (MPa)	t_m (ms)	$(dp/dt)_m$ (MPa/ms)	t (ms)
Original Sample	315.4	8.1	86.5	5.4
Impacted Sample	312.7	7.0	80.1	3.9

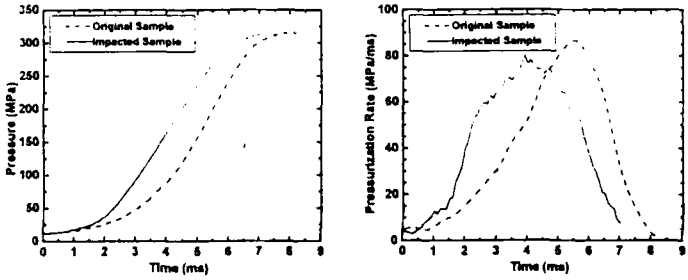

(a) (b)

Fig. 4 The Original and Impacted Samples (a) p-t Curves, (b) dp/dt-t Curves.

DDT TESTS

Experimental arrangements

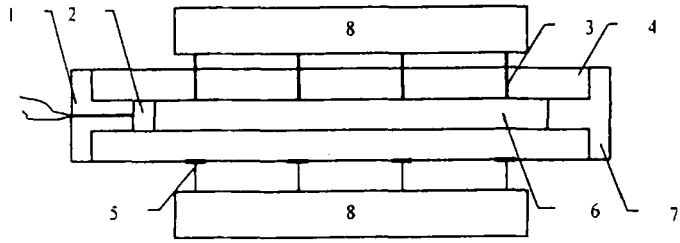

1. Igniter Bolt 2. Igniter 3. Optoelectronic Triode 4. Steel Tube
5. Strain Gauge 6. Charge Bed 7. End Closure 8. Oscilloscope

Fig. 5 Schematic of the Arrangement.

The DDT experimental arrangement is shown in Fig. 5. The arrangement is made up of a thick-walled steel tube (20mm inner diameter, 64mm outer diameter, 500mm length), closed at both ends with screw caps. In the tube, there are a 50mm igniter and a propellant charge bed 420mm long.

Both impacted and original samples were cut with a microtome into regular 5mm×5mm×5mm cubic grains. Then, 150g grains of the original or impacted propellants were put into each tube with a density of 1.076g/cm^3 (60%TMD), respectively.

The igniter consists of 1.5g NC (nitrocellulose) powders and an electric fuse. An electric fuse was heated by 30V DC voltage, then the charge bed was ignited.

Two kinds of gauges were distributed along the tube as shown in Fig. 5. Four optoelectronic triodes (model 3DU2D, response time 3.0μs) detected the passage of flame front, and another four strain gauges (BH350-4AA) detected the profiles of compacted/shocked waves. The signals were recorded with two TDS544A four-channel digital oscilloscopes (sample rate 1GS/s). Additionally, we also used 8 optoelectronic triodes, to survey the passage of the flame front in DDT.

Results and analyses

We list the results for four tests, test No.1 and No.3 are for the original propellant and test No.4 and No.6 for the impacted one. Parameters in tests and characteristic average velocity of waves are listed in Table 4-7 for tests No.1, 3, 6 and 4, respectively. Typical outputs of the optoelectronic triodes and strain gauges are given in Fig. 6 and Fig. 7 for tests No.1 and No.3. The two oscilloscopes were simultaneously triggered by the igniting voltage of the electric fuse. Hence, the initial time t=0 is the moment the fuse ignited. The legends in insets indicate the locations of gauges along the charge bed. The starting points are all the interfaces between the igniter and the charge. The base voltages of all signals are zero. For clarity, some were moved upward. Fig. 8 shows the comparison of distance-time and velocity-time plots of waves for original (test No.3) and impacted (test No.4) propellants.

For the original propellants, the experimental results are listed in Table 4 and Table 5. The typical signal curves are presented in Fig. 6 and Fig. 7. If one turns to Fig. 8(a), DDT is more clearly seen. The acceleration of flame fronts, as shown in Fig. 8(a), obviously

indicates a DDT and has been explained by many authors (see e. g. Ref. [6,7]).

Let us have a close look at DDT. In the pre-ignition stage, 1.5g NC was ignited to form a very slow burning event and to generate high-temperature product gas. The product gas, confined in the thick-walled steel tube, compressed the porous charge bed and ignited the charge bed. The ignition spreads slowly, Fig. 7. Moreover, the first signal (2.5cm) rose slowly, indicating convective burning had started. This was called the ignition/conductive burning stage. Generally, these two stages took up the greater part of time in DDT. The ignition spreads slowly. In the convective burning stage, due to the porosity of charge bed, high-temperature gas may penetrate into the unreactive charge bed. Then the unreactive bed was heated and ignited. In the third stage (compressive stage), the burning rate increased fast from about 0.09km/s between 2.5cm and 9.5cm to 0.2km/s between 9.5cm to 16.5cm (see Table 5). In Fig. 7(a), the third signal (16.5cm) rose slightly at about 13.6ms and changed fast at 13.9ms. At this stage a plug had formed in the compressed porous charge bed. Its width was approximately 6cm. From then on, the compressive burning rates increased continuously. Finally, within 34.5cm and 37.0cm, compressive waves formed a deflagration/low-speed detonation with a speed of 1.09km/s.

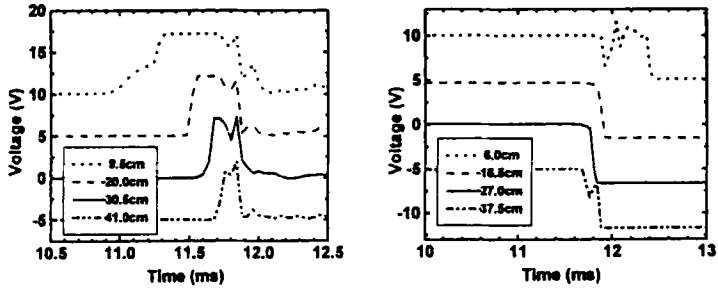

(a) (b)

Fig. 6 (a) Optoelectronic Triode Curves, (b) Strain Gauge Curves of Test No.1.

Table 4. Result of Test No.1.

	Optoelectronic triodes				Strain gauges			
Distance/cm	9.5	20.0	30.5	41.0	6.0	16.5	27.0	37.5
Time/ms	10.92	11.48	11.60	11.68	11.88	11.84	11.76	11.68
Distance interval/cm	10.5		10.5	10.5	10.5		10.5	10.5
Time interval/ms	0.56		0.12	0.08	-0.04		-0.08	-0.08
Average velocity /km/s	0.19		0.88	1.31	-2.60		-1.31	-1.31

As shown in Fig. 6 and Table 4, the response time of earlier signals of strain gauges fell behind those of optoelectronic triodes. Moreover, the data of strain gauges indicate that the wave accelerated backward. The fragments of the steel tube indicate that deflagnation/low-speed detonation did happen in test No.1.

Table 5. Result from Optoelectronic Triodes of Test No.3.

Distance /cm	2.5	9.5	16.5	23.5	30.5	34.0	37.5	41.0
Time /ms	12.468	13.216	13.564	13.694	13.802	13.844	13.876	13.914
Distance interval /cm	7.0		7.0	7.0	7.0	3.5	3.5	3.5
Time interval /ms	0.748		0.348	0.130	0.108	0.042	0.032	0.038
Average velocity /km/s	0.09		0.20	0.54	0.65	0.83	1.09	0.92

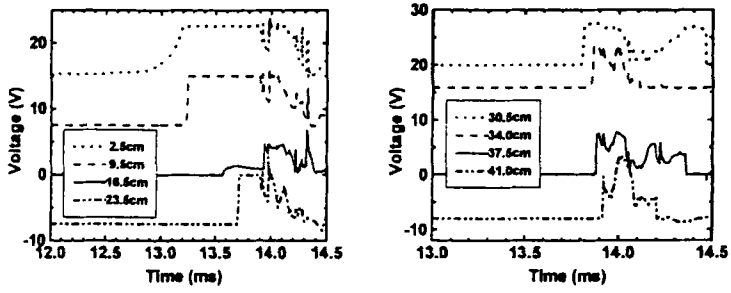

(a) (b)

Fig.7 (a) and (b) Optoelectronic Triode Curves of Test No.3.

For the impacted propellant, Experimental data are listed in Table 6 and Table 7. The DDT mechanism of the impacted propellant is basically the same as the original propellant. However, there are two salient differences. (1) In Fig. 8(a), to facilitate

comparison, the initial time t=0 in both test No.3 and test No.4 are shifted to the arrival time of flame front at location distance 2.5cm. From Fig. 8(a) and (b), the burning rate of the impacted propellant is faster than that of the original propellant. Moreover, a steep increase of the burning rate showed that a stronger wave had formed near 23.5cm. Actually, detonation took place (v=6.56km/s), see Test No.6 in Table 6. (2) The fragments from test No.4 and No.6 steel tubes are smaller than those formed by the detonation of the original propellant. The two differences indicate that damaging the propellant would increase its burning rate, and so might cause a hazard.

Table 6. Result of Test No.6.

	Optoelectronic triodes						Strain gauges			
Distance /cm	2.5	6.0	13.0	16.5	23.5	27.0	2.5	13.0	23.5	34.0
Time /ms	9.844	10.502	11.350	11.466	11.500	11.510	11.608	11.498	11.448	11.462
Distance interval /cm	3.5	7.0	3.5	7.0	3.5		10.5	10.5	10.5	
Time interval /ms	0.658	0.848	0.116	0.034	0.010		-0.112	-0.050	0.016	
Average velocity /km/s	0.05	0.08	0.30	2.06	3.50		-0.94	-2.10	6.56	

Table 7. Result from Optoelectronic Triodes of Test No.4.

Distance /cm	2.5	9.5	16.5	23.5	30.5	34.0	37.5	41.0
Time /ms	10.158	11.136	11.262	11.332	11.350	11.358	—	—
Distance interval /cm	7.0	7.0	7.0	7.0	3.5	3.5	3.5	
Time interval /ms	0.978	0.126	0.070	0.018	0.008	—	—	
Average velocity /km/s	0.07	0.56	1.00	3.89	4.38	—	—	

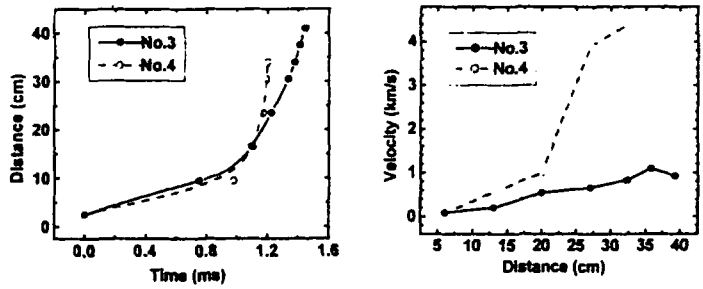

(a) (b)

Fig.8 Comparison from the Original (Test No.3) and Impacted (Test No.4) propellants

CONCLUSIONS

(1) This propellant can undergo extensive elastic deformation. It is a very viscoelastic material.

(2) In comparison with the microstructure of the original sample, there are two kinds of changes in the impacted sample: matrix tearing and the bigger RDX particles dewetting. These changes greatly enhance surface area. Moreover, measuring the changes of density can be used to quantify the damage.

(3) The DSC tests verified that the destruction of nitrate ester reduces its activation energy. Simultaneously, the reduced activation energy can increase the mass loss in TG tests.

(4) In closed-bomb tests, the apparent burn rate of the impacted sample varies considerably. Namely, increasing the burning surface may increase its burn rate. The results suggest that the burn rate differences shown the impacted sample is dependent on a surface area increase from the damage.

(5) The DDT results, for example tests No.3 and No.4, clearly show the influence of damage on DDT. This should be attributed to the higher surface to volume ratio of damaged propellant. In order to reduce the likelihood of DDT, the mechanical properties of a propellant should be improved to restrain its damage.

(6) Optoelectronic triodes are an effective and reliable way of making these measurements. Under certain circumstances (e. g. the above tests), ionization probes did not respond in the initial burning stages and optical fiber assemblies were too complicated. In our tests optoelectronic triodes provide relatively reliable, inexpensive and simple recordings of flame propagation.

Overall, the above results indicate that damage induced by impact could result in an increase in thermal decomposition and burn rate. In the worst case, it is possible that damage can lead to a deflagration-to-detonation transition (DDT).

In this paper, we investigated the effects of damage on decompositions of NEPE propellant. In the future, the aim is to develop a predictive model to describe the sensitivity of the NEPE propellant to damage.

ACKNOWLEDGEMENTS

This research was supported by the National Natural Science Foundation of China under Grant No.10102021 and No. 10172086.

REFERENCES

[1] Kang, J., Butler, P. B., and Baer, M. R., *Combustion and Flame* 89: 117-139(1992)

[2] James, E., DE93-018914

[3] Jean Lemaitre, *A Course on Damage Mechanics*, Springer-Verlag, 1992

[4] Li Li, Zhao Fengqi, Li Shangwen, Su Yanling, Dong Chunsheng, *Chinese Journal of Explosives & Propellants* 22(3): 11-14(1997)

[5] Luo Shanguo, Chen Futai, Tan Huimin, *Chinese Journal of Explosives & Propellants* 22(1): 22-26(1999)

[6] R. R. Bernecker, H. W. Sandusky and A. R. Clairmont. *Eighth Symposium (Int.) on Detonation*, Albuquerque, 1985:658-668

[7] Sandusky, H. W. and Bernecker, R. R., *Eighth Symposium (Int.) on Detonation*, Albuquerque, 1985:631-640